Electron temperature evolution in the plasma core of the TJ-II stellarator during and after cryogenic and TESPEL pellet injection

K. J. McCarthy[1], N. Tamura[2], J. L. Velasco[1], N. Panadero[1], I. García-Cortes[1], V. Tribaldos[3], E. Blanco[1], J. M. Fontdecaba[1], J. Hernández Sánchez[1], P. Medina[1], E. Pawelec[4], and TJ-II team[1]
[1]*Laboratorio Nacional de Fusión, CIEMAT, Madrid, Spain*
[2]*National Institute for Fusion Science, Toki, Gifu, 509-5292, Japan*
[3]*Universidad Carlos III de Madrid, Leganes, Madrid, Spain*
[4]*Institute of Physics, Opole University, Opole, Poland*

Introduction

Pellet injection is widely used in magnetically confined plasmas for core fuelling and impurity transport studies. When an injected cryogenic pellet enters the plasma, it is ablated by background plasma particles and the resultant ablated material forms a cloud of neutral and partially ionized particles that shields the pellet thereby giving rise to a self-regulated process [1]. Pellet databases [2] show that while penetration is dependent on electron density as well as on pellet mass and velocity, it is most sensitive to plasma electron temperature, T_e. In this work, made in the TJ-II stellarator, comparative studies using cryogenic and tracer-encapsulated solid pellets (TESPEL's) highlight unexpected perturbations in core T_e during and after both types are injected into microwave (ECRH), but not NBI, heated plasmas. The implications of such perturbations for pellet penetration are discussed.

Experimental set-up

The TJ-II is a 4-period heliac-type stellarator with a major radius of 1.5 m, a bean-shaped plasma cross-section, with an average minor radius of ≤0.22 m and a magnetic field B(0) ≤1 T. It is designed to explore a wide rotational transform range ($0.9 \leq \iota(0)/2\pi \leq 2.2$) in low, negative shear configurations ($\Delta\iota/\iota$ <6%) [3]. Plasmas, created with hydrogen, are heated using 2 gyrotrons operated at 53.2 GHz, the 2nd harmonic of the electron cyclotron resonance frequency (P_{ECRH} ≤600 kW, t ≤300 ms), so central electron densities, $n_e(0)$, and temperatures, $T_e(0)$, up to 1.7×10^{19} m^{-3} and 1 keV, are attained, respectively. In addition, two neutral beam injectors (NBI's) are operated and provide up to 1 MW (E_{beam} ≤32 keV) for ≤100 ms. As a result, plasmas with $T_e(0)$ ≤400 eV and $n_e(0)$ ≤5×10^{19} m^{-3} can been attained.

A pipe-gun type cryogenic pellet injector (PI) was developed and built at the laboratories of the Fusion Energy Division of Oak Ridge National Laboratory, Tennessee, USA before being installed on TJ-II. It consists of a gun box, in which up to 4 pellets are created, equipped with a gas propellant system for pellet acceleration. In this way, pellets, containing between 5×10^{18} and 4×10^{19} hydrogen atoms, achieve velocities between 800 and 1200 m/s [3]. Closer to TJ-II, the injection lines are equipped with a) light emitting diodes and light

sensitive diodes (light gates) and b) a microwave cavity detector (μwC). These provide timing signals while the μwC produces a mass dependent signal that allows particle accountability.

During a recent TJ-II experimental campaign, a cryogenic pellet formation pipe and its gas propulsion system were removed from the PI gun box to allow the direct rear-end coupling of a TESPEL system to it, thereby taking advantage of the PI in-line timing, gas expansion and vacuum systems [4]. For this, TESPEL's with outer and inner diameters of ~300 μm and 100 μm, respectively, were injected using an independent gas propulsion system (velocities from 125 to 300 m/s were achieved). Aluminium was selected as the tracer material so particle amounts were 6.7×10^{17} atoms (of both carbon and hydrogen) from the polystyrene shell plus 3.2×10^{16} aluminium atoms (providing 4.4×10^{18} and 4.1×10^{17} electrons from the shell and tracer, respectively). Some empty TESPEL's were also injected. Note: all injections are from the low magnetic field side of the plasma.

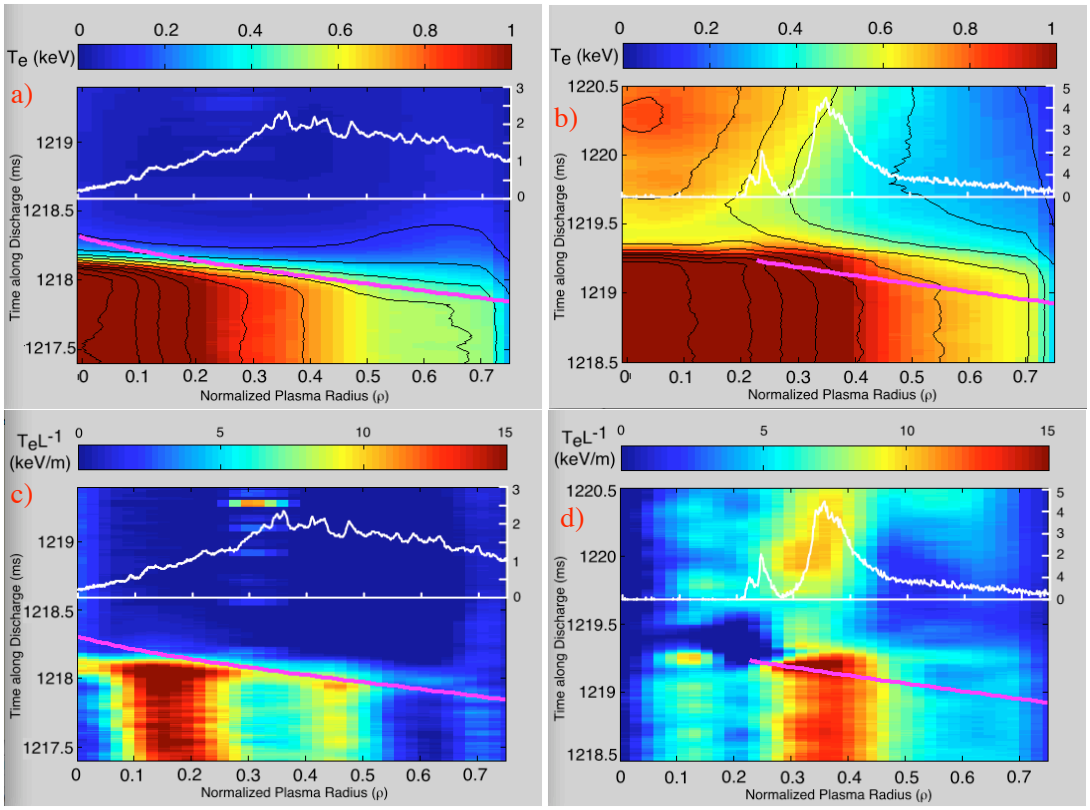

Figure 1: T_e profile evolution before and after TESPEL injection for discharges a) 40383 and b) 40506. c) and d): T_eL^{-1} gradients for same discharges. Hα light (10^{20} photons/s), which is proportional to ablation rate, along the plasma normalized radius is shown (white). Continuous lines represent TESPEL position as a function of time. Plasma and TESPEL parameters are similar for both cases. Constant value contours are in black.

In order to follow pellet ablation across the plasma minor radius, Balmer Hα (λ = 656.28 nm) and/or Al I (λ = 400 nm) light, emitted from the neutral cloud surrounding a pellet, is recorded using optical fibre based diagnostic systems installed outside nearby upper (TOP) and rear (SIDE) optical viewports. Other plasma parameters are followed using a range of

diagnostics that includes Thomson Scattering (TS), a microwave interferometer, and an 11 channel Electron Cyclotron Emission (ECE) system (both with 10 μs resolution), located 180º, 90º and 145º toroidally, respectively, from the PI.

Results

In TESPEL injections into low-density plasmas created with on-axis ECRH, and the standard magnetic configuration (100_44_64), a cooling front travels ahead of the slow 300 μm TESPEL if the outer T_e gradient, T_e L^{-1}, is <~5 keV/m, *i.e.* the plasma core cools before the TESPEL reaches it. See Fig. 1. Typically, this cold front travels at ~400 m/s in front of the ablating TESPEL. In contrast, when T_e L^{-1} >~5 keV/m for ρ >0.5, *e.g.* for off-axis ECRH (at ρ = 0.35), plasma cooling coincides with, or is delayed with respect to, TESPEL radial position. Similar cooling waves have sometimes, but not always, been reported in other devices [5, 6]. Therein, the plasma/experimental conditions that give rise to such a wave were not identified. Here, the main consequence of such a cooling wave is to provoke a strong central T_e collapse that extends significantly the TESPEL penetration depth, *i.e.* to beyond the TJ-II plasma centre, see Fig. 1. At present, the underlying physics remains to be determined.

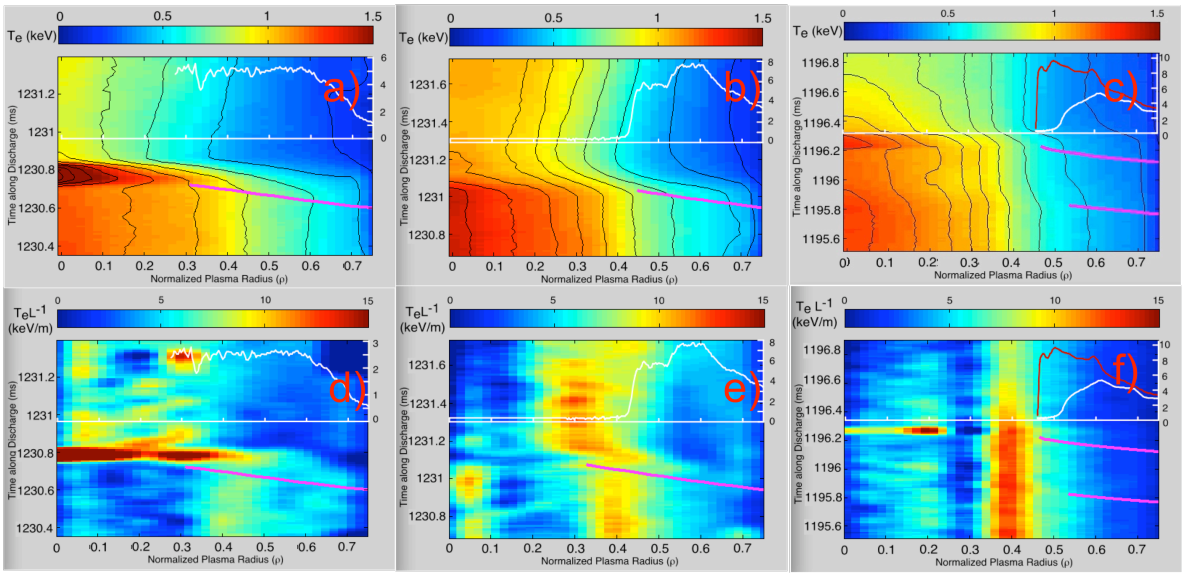

Figure 2: T_e profile evolution before and after pellet injection for discharges a) 41008, b) 41002 and c) 40231. d), e) and f): T_e gradient evolution for the same discharges. In c) and f) 2 pellets are injected. The Hα light collection rate (10^{20} photons/s), proportional to ablation rate, across the plasma normalized radius is shown (white & maroon). Continuous lines represent pellet position as a function of time. Plasma and pellet (5×10^{18} H) parameters are similar for all, except for the 2nd pellet in c) (9×10^{18} H). Constant value contours are in black.

In the case of the fast cryogenic pellets (≤1200 m/s) a cold front is not observed (the high pellet speed could be masking this effect). Rather a transitory (≤~100 μs), but significant, rise in core T_e is observed immediately after the pellet has travelled towards the plasma centre in some (Fig. 2a & 2c), but not all (Fig. 2b), of the ECRH plasmas reviewed to date. Moreover, closer examination of Fig. 2, reveals that this perturbation begins close to ρ = 0 and moves

outwards. A similar T_e rise is seen in some TESPEL injections, even if the TESPEL is preceded by an inward moving cold front. From Fig. 2a and similar discharges, it is noted that a strong core T_e rise ($\rho < 0.3$) is triggered when a pellet penetrates beyond $\rho = 0.45$ causing a significant local change in T_eL^{-1} ($\rho = 0.3$ to 0.45). However, for shallower pellet penetrations, it is not so obvious. In some cases, this core T_e increase is not seen. See Fig. 2b and the 1st pellet of Fig. 2c. In contrast, for the 2nd pellet in Fig. 2c, which penetrates to $\rho = 0.45$, a small but significant core T_e occurs even though T_eL^{-1} is larger than in the other cases. It should also be noted that during short time period the bulk plasma density remains unchanged as pellet particles remain local to the injection sector [3], while the ECE diagnostic is located 145º toroidaly from the PI. Thus, it appears that T_eL^{-1} and pellet penetration are involved in this second effect. Finally, the development of core T_e spikes was observed in previous TJ-II experiments that involved edge-cooling pulses (nitrogen gas injection) [7].

Discussion

The implication of a pre-cooling front on pellet penetration and central T_e collapse has been observed. Its trigger appears to be linked to T_e gradient, though the physical background remains unclear. In contrast, a significant, but transitory ($\leq$100 μs), rise in core T_e is noted during and immediately after injection under certain ECRH plasma conditions. Although at present the trigger mechanism is unclear, it is postulated that pellet injection may temporally improve electron energy confinement: a local increased radial T_e gradient caused by ablation leads to a more positive radial electric field (E_r). Thus the plasma may move deeper into Core Electron Root Confinement, a regime of reduced neoclassical transport [8]; the associated larger E_r shear could also contribute to reduce electron energy turbulent transport [9]. This improvement of confinement could cause the temporary observed T_e rise. However, since the T_e gradient is not sustained (see Fig. 2a), it reduces and the core T_e collapses quickly.

This work has been carried out within the framework of the EUROfusion Consortium and has received funding from the Euratom research and training programme 2014-2018 under grant agreement No 633053. The views and opinions expressed herein do not necessarily reflect those of the European Commission. It is also partially financed by the Spanish Ministerio de Ciencia y Innovación (ENE2013-48679-R) and by NIFS/NINS under the Formation of International Scientific Base and Network project. N.T. acknowledges support from the Fusion-EP Scholars Program.

[1] B. Pégourié, Plasma Phys. Control. Fusion 49 (2007) R87.
[2] L. R. Baylor et al., Nucl. Fusion 37 (1997) 445.
[3] K. J. McCarthy et al., Proc. Sci. (ECPD2015) 134.
[4] N. Tamura et al., Rev. Sci. Instrum. (2016) to be published.
[5] Equipe TFR, *Plasma Phsics and Controlled Nuclear Fusion Research 1984: Proc. 10th Int. Conf. (London 1984)* vol 1 (Vienna: IAEA) p 103.
[6] L. Ledl et al., Nucl. Fusion 44 (2004) 600.
[7] B. van Milligen et al. Nucl. Fusion 42 (2002) 787.
[8] M. Yokoyama et al., Nucl. Fusion 47 (2007) 1213.
[9] K. Ida et al, Phys. Rev. Lett. 76 (1996) 1268.